Liquid Crystals
Publication details, including instructions for authors and subscription information:
http://www.informaworld.com/smpp/title~content=t713926090

A molecular theory including hard rod interactions of liquid crystalline phases exhibited by highly polar compounds

A. S. Govind[a]; N. V. Madhusudana[b]
[a] Department of Physics, Vijaya College, Basavanagudi, Bangalore 560 004, India, [b] Raman Research Institute, C.V. Raman Avenue, Bangalore 560 080, India,

To cite this Article Govind, A. S. and Madhusudana, N. V.(2000) 'A molecular theory including hard rod interactions of liquid crystalline phases exhibited by highly polar compounds', Liquid Crystals, 27: 9, 1249 — 1258

To link to this Article: DOI: 10.1080/02678290050122114

URL: http://dx.doi.org/10.1080/02678290050122114

LIQUID CRYSTALS, 2000, VOL. 27, NO. 9, 1249–1258

A molecular theory including hard rod interactions of liquid crystalline phases exhibited by highly polar compounds

A. S. GOVIND
Department of Physics, Vijaya College, Basavanagudi, Bangalore 560 004, India

and N. V. MADHUSUDANA*
Raman Research Institute, C.V. Raman Avenue, Bangalore 560 080, India

(*Received 15 September 1999; in final form 3 April 2000; accepted 7 April 2000*)

We extend our molecular mean field model of highly polar compounds to include hard rod interactions to develop a hybrid model. The latter interactions are restricted to second virial terms, following a method developed by Koda and Kimura. This allows us to calculate pressure–temperature phase diagrams. Depending on the model parameters used, the phase diagrams exhibit the following features: nematic–nematic phase transition, bounded $\mathrm{SmA_d}$ region, double reentrance, reentrant nematic lake surrounded by the smectic A phase (the reentrant nematic lake merging with the main nematic sea) as well as the possibility of quadruple reentrance. We compare the calculated phase diagrams with the available experimental data.

1. Introduction

In this paper, we consider liquid crystals composed of rod-like molecules. The nematic (N) liquid crystal has a long range orientation order of the long axes of molecules and no long range translational order. The smectic A (SmA) liquid crystal has an additional quasi long range one-dimensional translational order parallel to the long axes of molecules, i.e. a layering order with a spacing d. The smectic phase is favoured if the molecules have relatively long aliphatic chains. Usually the layer spacing is of the order of molecular length l. The usual sequence of phase transitions on cooling from the isotropic liquid (I) phase is I → N → SmA → Cr (crystal). However, if the molecules have a strong longitudinal electric dipole moment due to cyano or nitro end groups, different molecular associations are possible, resulting in smectic phases with $d \neq l$. The SmA phase is termed as $\mathrm{SmA_1}$ phase if $d \approx l$, whereas it is a $\mathrm{SmA_d}$ phase if $l < d < 2l$. Liquid crystals composed of highly polar molecules are known to exhibit a variety of unusual phase sequences such as double re-entrance, smectic $\mathrm{A_1}$–smectic $\mathrm{A_d}$ transition [1], etc. Studies on reentrant liquid crystal have been recently reviewed by Cladis [2].

These phenomena have been successfully explained on the basis of a Landau theory by Prost and coworkers [3, 4]. In this model, two competing order parameters are used to describe such media. The two order parameters correspond to two incommensurate lengths, namely the molecular length l and the length l' of a suitably associated antiparallel pair of molecules such that $l < l' < 2l$.

There have also been several attempts to develop molecular theories of the phase transitions in highly polar compounds [5–14]. A particularly simple model was proposed by us to explain double reentrance [12] and other unusual phase transitions [13–15]. In this model [12] the molecular origin of the *two lengths* is explained as follows: the interaction between permanent dipoles favours an antiparallel orientation (A) between neighbouring molecules [16]. The interaction energy is $\propto 1/r^3$ where r is the intermolecular separation. The aromatic part of the antiparallel neighbours overlap due to strong anisotropic dispersion interaction between them and a tendency for the aromatic and aliphatic parts to segregate. This results in the well known partial bilayer structure, figure 1 (*a*).

On the other hand, if the polar molecules are parallel, the dipole interaction is repulsive. However, in view of the strong polarizability of the conjugated aromatic core to which the dipole is attached, the latter induces an oppositely oriented dipole moment in the neighbouring molecule, thus reducing the net dipole moment of each molecule, figure 1 (*b*). Further, in this 'parallel' (or P) configuration, the chains are in close proximity, adding

---

*Author for correspondence; e-mail: nvmadhu@rri.ernet.in

Liquid Crystals ISSN 0267-8292 print/ISSN 1366-5855 online © 2000 Taylor & Francis Ltd
http://www.tandf.co.uk/journals

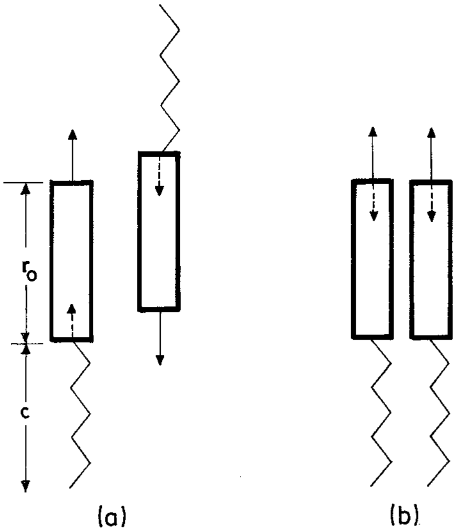

Figure 1. Schematic diagram showing the mutual configuration in antiparallel (*a*) and parallel (*b*) pairs of molecules. The solid arrow represents the permanent dipole; and dotted arrow represents the induced dipole.

to the attractive interaction. Both these interaction energies are $\propto 1/r^6$. Hence, one can expect a change in the configuration of the pairs from 'A' type to 'P' type as the intermolecular separation is decreased below some value as the density is increased due to the lowering of temperature or increase of pressure. This implies the existence of a polar short range order at low temperatures. Indeed such a polar short range order has been experimentally detected by us recently [17], thus supporting the basic idea of our model. Using extensions of this model, we have explained the nematic–nematic and SmA_1–SmA_d transitions, the occurrence of the reentrant nematic lake, the effect of an external electric field on the phase diagram, etc. [13–15].

The difference in the configurational energy ($\Delta\varepsilon$) between antiparallel and parallel pairs is a sensitive function of the intermolecular separation and hence the density. However, as the temperature is lowered across the temperatures corresponding to the stability of reentrant phases, the density increases monotonically [18]. Hence for the sake of simplicity, in our earlier discussions [12–15] we assumed $\Delta\varepsilon$ to be a function of temperature.

Several experimental investigations have also been carried out on the phase diagrams of such liquid crystals as functions of pressure. In particular, the SmA_d phase becomes bounded in the *p*–*T* plane and the SmA_1–reentrant nematic transition temperature increases monotonically with pressure [18, 19]. High pressure studies on the reentrant phases exhibited by the binary mixtures of hexyloxycyanobiphenyl (6OCB) and its higher homologue (8OCB) were reported long ago [18] and the SmA_d phase is seen to be more stable for mixtures with higher concentrations of the higher homologue. To explain such phase diagrams theoretically, an explicit calculation of pressure is desirable. For this purpose, packing effects which take into account the hard rod features of molecules have to be considered. Even though many experimental investigations have been carried out on the *p*–*T* phase diagrams, there is no detailed molecular theory of such phenomena. A thermodynamic theory has been developed by Clark [20]. Indekeu and Berker have developed a spin gas model [6], in which the pressure is simply assumed to be proportional to the inverse of molecular separation. Recently Sear and Jackson [21], have developed a hard rod model of a binary mixture consisting of interconverting monomers and dimers following the method of Koda and Kimura [22]. In this model, the temperature is introduced through the equilibrium constant in the monomer–dimer potential and the calculation is restricted to the packing fraction–temperature phase diagrams. In the present paper, we extend our mean field model of highly polar compounds [13] to include the hard rod features and develop a hybrid model. This allows us to calculate different phase diagrams as functions of pressure.

Several hard rod models of liquid crystals have been developed over the past decades. Onsager [23] was the first to show that packing effects alone can stabilize the nematic phase in the case of long rod-like molecules with aspect ratios ~ 100. However, extension of the hard rod models to smectic liquid crystals is not straightforward. In fact from computer simulations [24], it is known that a system of hard ellipsoids does not form a smectic phase due to packing effects alone. On the other hand, computer simulation studies [24], experiments [25] and a few specific theoretical models [26–29], show that a system of hard *spherocylinders* can form the nematic and smectic A phases. As explained by Wen and Meyer [28], the SmA phase in this case is stabilized because the loss of entropy in the formation of layering order is more than compensated by the gain in entropy due to the increased freedom of molecules within the layers.

In our model of polar compounds, the medium is assumed to be a *mixture* of antiparallel and parallel pairs [12–15]. Thus we have to consider hard rod models of binary mixtures [30, 22] to extend our model. The relative concentration of antiparallel and parallel pairs is not a constant, but varies with both temperature and pressure making the calculations quite tedious. Hence, in the present paper we adopt the relatively simple theory of hard rod mixtures developed by Koda and Kimura for molecules with perfect orientational order and extend it to develop a hybrid model for the nematic–smectic transitions in liquid crystals with molecules having strong dipole moments. We express $\Delta\varepsilon$ as a function of density, i.e. packing fraction, and calculate pressure explicitly. We calculate the phase diagrams as functions of pressure. Depending on the parameters used, the calculations yield one or more of the following features: nematic–nematic phase transition, bounded SmA_d region, double reentrance, reentrant nematic lake surrounded by the smectic A (the reentrant nematic lake merging with the main nematic sea) and also the possibility of quadrupole reentrance. These are compared with available experimental data. The inclusion of hard rod features leads to the following new results: (a) explicit calculation of pressure, (b) effect of chain length on the *p–T* phase diagram, and (c) realization of N_1–N_d and SmA_1–SmA_d transitions even in the absence of deviation from the geometric mean rule in the attractive interactions. The model provides a molecular basis for the two lengths introduced by Prost in the phenomenological Landau theory [1, 4].

In § 2, the theoretical model is developed. In § 3, various calculated phase diagrams as functions of pressure are presented and discussed in comparison with experimental data. Some concluding remarks are given in § 4.

2. Theoretical model

2.1. *Assumptions*

First, we assume the medium to be a binary mixture of parallel (P) and antiparallel (A) types of dimers. For the sake of notational convenience, we indicate the former by the suffix '1' and the latter by '2'. The configurational energy difference is given by

$$\Delta\varepsilon = \varepsilon_2 - \varepsilon_1 = A k_B T^* \left(\frac{\eta}{\eta^*} - 1\right) \tag{1}$$

where A is a dimensionless interaction parameter, k_B the Boltzmann constant, T^* some reference temperature, η the packing fraction and η^* is the packing fraction at which $\varepsilon_2 = \varepsilon_1$. For $\eta > \eta^*$, $\Delta\varepsilon$ is positive which means that ε_1 is more negative than ε_2 and the P type configuration is favoured over the A type configuration.

Second, both A and P types of dimers are assumed to be right circular cylinders of the same volume v, but of different lengths l_2 and l_1 respectively ($l_2 > l_1$) and the corresponding diameters are denoted by D_2 and D_1. We define

$$q = \frac{l_2}{l_1} = \frac{D_1^2}{D_2^2}. \tag{2}$$

The packing fraction is given by

$$\eta = \frac{N_1 v + N_2 v}{V} = \frac{N v}{V} \tag{3}$$

where N_1 and N_2 are the number of P and A types of pairs respectively, V is the system volume, $v = \pi D_1^2 l_1/4 = \pi D_2^2 l_2/4$ and $N = N_1 + N_2$ is the total number of pairs. The volume fractions which are the same as the relative fractions of P and A types of pairs respectively are

$$x_1 = \frac{N_1}{N}, \qquad x_2 = \frac{N_2}{N} \tag{4}$$

such that $x_1 + x_2 = 1$.

Third, most of the phenomena like reentrance occur well below the nematic–isotropic transition temperature. Hence for simplicity, especially in the calculation of excluded volume effects, the cylinders are assumed to have perfect orientational order and aligned along the Z-axis.

2.2. *Free energy*

2.2.1. *Hard rod component*

The hard rod part of the Helmholtz free energy F^h is calculated in the second virial approximation following Koda and Kimura [22]. Let $P_v(\mathbf{r})$ be the packing fraction of cylinders of length l_v at the position $\mathbf{r} = (x, y, z)$. Obviously $\int_V d\mathbf{r}\, P_v(\mathbf{r}) = N_v v$, the fractional volume occupied by the species of the type v (= 1 or 2).

F^h can be expressed as a functional of $P_v(\mathbf{r})$ in the form

$$\frac{F^h}{k_B T} = \sum_v N_v A_v(T) + \sum_v \frac{1}{v} \int_V d\mathbf{r}\, P_v(r) \ln P_v(\mathbf{r}) - \frac{1}{2} \sum_v \sum_{v'} \frac{1}{v^2} \int_V d\mathbf{r}_1\, d\mathbf{r}_2\, P_v(\mathbf{r}_1) P_{v'}(\mathbf{r}_2) b_{vv'}(\mathbf{r}_1, \mathbf{r}_2) + \{\text{higher order terms in } P_v(\mathbf{r})\} \tag{5}$$

where T is the temperature, $A_v(T)$ which is a function of only T is the contribution from kinetic energy, and the Meyer function $b_{vv'}(\mathbf{r}_i, \mathbf{r}_j)$ for parallel cylinders is given by

$$b_{vv'}(\mathbf{r}_i, \mathbf{r}_j) = -H\left[\left(\frac{l_v + l_{v'}}{2}\right)^2 - (z_i - z_j)^2\right] \times H\left[\left(\frac{D_v + D_{v'}}{2}\right)^2 - (x_i - x_j)^2 - (y_i - y_j)^2\right] \tag{6}$$

where $H(a) = 0$ for $a \leqslant 0$ and $H(a) = 1$ for $a > 0$ and the Z-axis is taken along the nematic director.

The packing fraction of each kind of cylinder is uniform in the nematic phase and is given by

$$P_v(\mathbf{r}) = \frac{N_v v}{V} \tag{7}$$

while that in the SmA phase is a periodic function of z, i.e. [22]

$$P_v(\mathbf{r}) = \frac{N_v v}{V} \rho_v(z). \tag{8}$$

We define $\zeta = z/l_1$, i.e. take l_1 as unit of length. Substituting equations (6) and (8) into equation (5) and neglecting higher order terms, we can write the free energy per pair

$$f^{\mathrm{h}} = \frac{F^{\mathrm{h}}}{Nk_{\mathrm{B}}T} \tag{9}$$

as a functional of $\rho_v(\zeta)$ as:

$$\begin{aligned}
&f^{\mathrm{h}}[\rho_1(\zeta), \rho_2(\zeta)] \\
&\quad = x_1\left[\Lambda_1(T) + \ln \frac{N_1 v}{V}\right] + x_2\left[\Lambda_2(T) + \ln \frac{N_2 v}{V}\right] \\
&\qquad + \frac{x_1}{L}\int_L \mathrm{d}\zeta\, \rho_1(\zeta) \ln \rho_1(\zeta) + \frac{x_2}{L}\int_L \mathrm{d}\zeta\, \rho_2(\zeta) \ln \rho_2(\zeta) \\
&\qquad + 2x_1^2\eta\frac{1}{L}\int_L \mathrm{d}\zeta\, \mathrm{d}\zeta'\, \rho_1(\zeta)\rho_1(\zeta')H[1-(\zeta-\zeta')^2] \\
&\qquad + 2x_2^2\eta\frac{1}{qL}\int_L \mathrm{d}\zeta\, \mathrm{d}\zeta'\, \rho_2(\zeta)\rho_2(\zeta')H[q^2-(\zeta-\zeta')^2] \\
&\qquad + x_1x_2\eta\left(1+\frac{1}{\sqrt{q}}\right)^2\frac{1}{L}\int_L \mathrm{d}\zeta\, \mathrm{d}\zeta'\, \rho_1(\zeta)\rho_2(\zeta') \\
&\qquad \times H\left[\left(1+\frac{q}{2}\right)^2-(\zeta-\zeta')^2\right]
\end{aligned} \tag{10}$$

where L is the system size along the Z-axis in units of l_1.

The sinusoidal perturbation of $\rho_v(\zeta)$ in smectic A can be written as

$$\rho_v(\zeta) = 1 + a_v \cos k\zeta \tag{11}$$

where $k = 2\pi/d$ is the (dimensionless) wavenumber of the perturbations with d as the average layer spacing in units of l_1, and a_v represent amplitudes equivalent to order parameters in smectic A. Substituting equation (11) into equation (10) and neglecting higher powers in a_1 and a_2, we can write,

$$f^{\mathrm{h}} = \frac{F^{\mathrm{h}}}{Nk_{\mathrm{B}}T} = f_{\mathrm{N}} + \delta f_{\mathrm{S}}^{\mathrm{h}}. \tag{12}$$

As the medium is assumed to have perfect orientation order, the nematic free energy per pair arises from the hard rod interactions and the pairing energy ($\Delta\varepsilon$). We have

$$\begin{aligned}
\frac{F_{\mathrm{N}}}{Nk_{\mathrm{B}}T} = f_{\mathrm{N}} &= x_1\left[\Lambda_1(T) + \ln \frac{N_1 v}{V}\right] \\
&\quad + x_2\left[\Lambda_2(T) + \ln \frac{N_2 v}{V}\right] \\
&\quad + \eta[4 + x_1x_2 b(q)] + x_2\frac{\Delta\varepsilon}{k_{\mathrm{B}}T}
\end{aligned} \tag{13}$$

where

$$b(q) = \left(1 + \frac{1}{\sqrt{q}} + \sqrt{q}\right)^2 - 9. \tag{13 a}$$

The smectic perturbation energy is,

$$\begin{aligned}
\frac{\delta F_{\mathrm{S}}^{\mathrm{h}}}{Nk_{\mathrm{B}}T} &= \delta f_{\mathrm{S}}^{\mathrm{h}} \\
&= x_1\frac{a_1^2}{4} + x_2\frac{a_2^2}{4} + 2x_1^2\eta a_1^2\frac{\sin k}{k} + 2x_2^2\eta a_2^2\frac{\sin qk}{qk} \\
&\quad + x_1x_2\eta\left(1+\frac{1}{\sqrt{q}}\right)^2\frac{a_1a_2}{k}\sin\left[\frac{k(1+q)}{2}\right].
\end{aligned} \tag{14}$$

Since the rods are assumed to be perfectly aligned, the SmA–N transition is second order in nature. Hence, at the transition point, x_v is the same in the SmA and N phases.

2.2.2. *Attractive component in the smectic phase*

The energy of ith pair in the smectic medium is given by

$$u_{iv} = -u_{\mathrm{o}}\eta\sum_{v'}\alpha_{vv'}x_{v'}a_{v'}\cos\left(\frac{2\pi\zeta_{iv}}{d}\right) \tag{15}$$

where u_{o} is an interaction parameter which is taken to be equal to 4.541 $k_{\mathrm{B}}T^*$, and $T^* = 500$ K would correspond to the N–I transition temperature if the nematic order parameter were not assumed to be saturated. $\alpha_{vv'}$ are the McMillan parameters defined as

$$\alpha_{vv} = 2\exp[-(\pi r_{\mathrm{o}}/d_{vv})^2] \tag{16}$$

and

$$\alpha_{vv'} = (\alpha_{vv}\alpha_{v'v'})^{1/2} \tag{17}$$

where $d_{11} = r_{\mathrm{o}} + c$ and $d_{22} = r_{\mathrm{o}} + 2c$, with r_{o} and c being the lengths of aromatic and chain moieties respectively (see figure 1). α_{22} is obviously related to α_{11}.

The total internal energy of N pairs is,

$$U = \frac{N}{2}\sum_v\langle u_{iv}\rangle x_v = -\frac{N}{2}u_{\mathrm{o}}\eta\sum_v\sum_{v'}\alpha_{vv'}x_vx_{v'}a_va_{v'} \tag{18}$$

where $\langle\ \rangle$ indicates statistical average and we have used

$$a_\nu = \left\langle \cos\left(\frac{2\pi\zeta_{i\nu}}{d}\right)\right\rangle = \int_0^1 \mathrm{d}\xi_\nu\, \phi_\nu \cos(\pi\xi_\nu) \qquad (19)$$

with $\xi_\nu = 2\zeta_\nu/d$ as the reduced coordinate and ϕ_ν is the normalized distribution function for the ν-type of pairs.

The entropy of N pairs is,

$$S = -Nk_\mathrm{B}\sum_\nu x_\nu \int_0^1 \mathrm{d}\xi_\nu\, \phi_\nu \ln\phi_\nu \qquad (20)$$

and therefore the attractive part of the *smectic* free energy in the mean field approximation for the medium with perfect orientational order is given by, $\Delta F_\mathrm{S}^\mathrm{a} = U - TS$,

$$\text{i.e. } \delta f_\mathrm{S}^\mathrm{a} = \frac{\Delta F_\mathrm{S}^\mathrm{a}}{Nk_\mathrm{B}T} = -\frac{u_\mathrm{o}\eta}{2k_\mathrm{B}T}\sum_\nu\sum_{\nu'}\alpha_{\nu\nu'}x_\nu x_{\nu'}a_\nu a_{\nu'} + \sum_\nu x_\nu \int_0^1 \mathrm{d}\xi_\nu\, \phi_\nu \ln\phi_\nu. \qquad (21)$$

2.2.3. *Free energy due to smectic ordering*

The free energy due to smectic ordering is given by

$$\delta f_\mathrm{S} = \delta f_\mathrm{S}^\mathrm{h} + \delta f_\mathrm{S}^\mathrm{a} = -x_1x_2a_1a_2\tilde{C} + \sum_\nu\left(-\frac{x_\nu a_\nu^2 C_\nu}{2} + x_\nu\int_0^1 \mathrm{d}\xi_\nu\, \phi_\nu\ln\phi_\nu\right) \qquad (22)$$

where we have defined,

$$C_1 = \left[\frac{u_\mathrm{o}}{k_\mathrm{B}T}\alpha_{11} - 4j_\mathrm{o}(k)\right]\eta x_1 - \frac{1}{2} \qquad (23)$$

$$C_2 = \left[\frac{u_\mathrm{o}}{k_\mathrm{B}T}\alpha_{22} - 4j_\mathrm{o}(qk)\right]\eta x_2 - \frac{1}{2} \qquad (24)$$

$$\tilde{C} = C_{12} = C_{21} = \left\{\frac{u_\mathrm{o}}{k_\mathrm{B}T}\alpha_{12} - \frac{1}{k}\left(1+\frac{1}{\sqrt{q}}\right)^2 \sin\left[\frac{k(1+q)}{2}\right]\right\} \qquad (25)$$

where $j_\mathrm{o}(m) = \sin(m)/m$ is the zeroth order Bessel function.

The distribution function ϕ_ν for the νth species is obtained by minimizing δf_S:

$$\phi_\nu = \frac{1}{Z_\nu}\phi_\nu^* = \frac{1}{Z_\nu}\exp[(a_\nu C_\nu + x_{\nu'}a_{\nu'}\eta\tilde{C})\cos\pi\xi_\nu] \qquad (26)$$

where ν' now represents the second species, and the partition function $Z_\nu = \int_0^1 \mathrm{d}\xi_\nu\, \phi_\nu^*$.

Substituting ϕ_ν in equation (22), we get

$$\delta f_\mathrm{S} = \sum_\nu\left(\frac{x_\nu a_\nu^2 C_\nu}{2} - x_\nu \ln Z_\nu\right) + x_1x_2a_1a_2\tilde{C}. \qquad (27)$$

Expanding $\ln Z_\nu$ and neglecting higher powers in a_1 and a_2, we get

$$\delta f_\mathrm{S} = (a_1 \quad a_2)\begin{pmatrix} S_{11} & S_{12} \\ S_{21} & S_{22}\end{pmatrix}\begin{pmatrix} a_1 \\ a_2\end{pmatrix} \qquad (28)$$

where

$$S_{11} = \frac{x_1}{4}(2C_1 - C_1^2 - x_1x_2\tilde{C}^2)$$

$$S_{22} = \frac{x_2}{4}(2C_2 - C_2^2 - x_1x_2\tilde{C}^2)$$

$$S_{12} = S_{21} = \frac{1}{2}x_1x_2\tilde{C}\left(1 - \frac{C_1 + C_2}{2}\right). \qquad (29)$$

$\delta f_\mathrm{S} = 0$ determines the N–SmA transition point. This condition is equivalent to

$$\det(S) = S_{11}S_{22} - S_{12}S_{21} = 0. \qquad (30)$$

Using equations (29) at the transition point, we get

$$x_1x_2\tilde{C}^2 - C_1C_2 = \varDelta = 0. \qquad (31)$$

2.3. *Expressions for k and x_2*

k can be found by minimizing δf_S given by equation (28). The value k_c at the transition is given by

$$k_\mathrm{c} = \frac{\left\{x_1x_2\tilde{C}\left(1+\frac{1}{\sqrt{q}}\right)^2 \sin\left[\frac{k_\mathrm{c}(1+q)}{2}\right] - 2C_1x_2\frac{\sin(qk_\mathrm{c})}{q} - 2C_2x_1\sin k_\mathrm{c}\right\}}{\left\{x_1x_2\tilde{C}\left(1+\frac{1}{\sqrt{q}}\right)^2\left(\frac{1+q}{2}\right)\cos\left[\frac{k_\mathrm{c}(1+q)}{2}\right] - 2C_1x_2\cos(qk_\mathrm{c}) - 2C_2x_1\cos k_\mathrm{c}\right\}}. \qquad (32)$$

In view of the assumption of saturated nematic order, the N–SmA transition is second order in nature and at the transition point $x_2 = x_2^\mathrm{N}$. Therefore x_2 is found by the condition $\partial F_\mathrm{N}/\partial x_2 = 0$. This gives

$$x_2 = \frac{1}{1 + \exp\left[\eta(1-2x_2)b(q) + \frac{\Delta\varepsilon}{k_\mathrm{B}T}\right]} \qquad (33)$$

2.4. *Expression for pressure*

We have $p = -(\partial F/\partial V)_T$. As above, at the N–SmA transition point, $p = p_\mathrm{N}$. Hence,

$$\frac{pv}{k_\mathrm{B}T} = -\left[\frac{\partial(F_\mathrm{N}v/k_\mathrm{B}T)}{\partial V}\right]_T.$$

Using equation (13) we get

$$\frac{pv}{k_B T} = \eta + \eta^2 \left[4 + \frac{x_2 A}{T_R \eta^*} + x_1 x_2 b(q) \right]. \qquad (34)$$

2.5. *Expression for Gibbs free energy*

We have, at the transition point the Gibbs free energy, $G = G_N = F_N + pV$. Therefore,

$$\frac{G_N}{N k_B T} = 1 + x_1 \left[A(T) + \ln\left(\frac{N_1 v}{V} \right) \right] + x_2 \left[A(T) + \ln\left(\frac{N_2 v}{V} \right) \right] + \eta \left\{ \frac{x_2 A}{T_R \eta^*} + 2[4 + x_1 x_2 b(q)] \right\} + \frac{x_2 \Delta\varepsilon}{k_B T}. \qquad (35)$$

2.6. *Method of calculation*

A given compound is characterized by the parameters A, η^*, q [see equations (1) and (2)] and α [see equation (16)]. Fixing the packing fraction η and the relative temperature T_R, the values of k and x_2 are found by self consistency of equations (32) and (33). With these values, Δ of equation (31) is calculated for η varying from zero to η_{max} (about 0.9 for hexagonal close packing of cylinders). $\Delta > 0$ corresponds to the smectic phase. The values of η corresponding to the N–SmA transition are located by the condition $\Delta = 0$. The transition pressures are calculated using equation (34). If x_1 is large, the smectic has monolayer order (i.e. SmA$_1$), otherwise it is SmA$_d$. The suffix 'R' in N$_R$, N$_{R1}$ and N$_{Rd}$ denotes a reentrant nematic phase. Within the nematic phase, even though we have assumed the order parameter $S = 1$, there can be a first order nematic to nematic transition involving a jump in x_1. At this transition the Gibbs free energies corresponding to the two phases having (η, x_1) and (η', x_1') at a particular pressure become equal. We denote the nematic with a larger (smaller) value of x_1 as the N$_1$ (N$_d$) phase.

3. Results and discussion

3.1. *Nematic to nematic transition*

We first discuss the nematic to nematic transition. For $\eta^* = 0.55$ and $q = 1.2$ the N–N transition lines are shown in the p–T plane in figure 2, for different values of A. The transition is from the N$_1$ phase (above the line) to the N$_d$ phase (below the line). It is seen that the N$_1$–N$_d$ transition temperature increases with pressure and the first order N$_1$–N$_d$ transition line ends in a critical point (p_c, T_c). The critical point shifts to higher values of (p, T) on increasing A which is proportional to $\Delta\varepsilon$, see equation (1). Thus, the possibility of observing such a transition increases for larger values of A. The value of A can be expected to increase with the dipole moment of the molecules. Indeed, while 7CB does not exhibit the N–N transition, the analogous molecule with an ester group dipole adding to that of the cyano group exhibits the transition [31]. Experimentally the transition temperature has an approximately linear dependence on pressure [32] as seen in figure 2. The value of A also increases with chain length in a homologous series as explained in [13]. The above calculations have been made with a fixed length ratio q. Actually, when the chain length is increased, both q and $\Delta\varepsilon$ increase. Near $q = 1.5$, if the chain length is increased by 50%, $\Delta\varepsilon$ increases by an order of magnitude [13], whereas q increases only by about 10%. Calculations show that an increase of q results in a stronger first order N$_1$–N$_d$ transition at a lower pressure for fixed values of other parameters. At the N$_d$–N$_1$ transition, the downward jump in x_2 is accompanied by a jump in η to higher values, resulting in a better packing at the same p and T values and this packing effect obviously depends on q. Hence, in general, as the chain length is increased, if the smectic phase does not intervene, the first order nature of the N$_1$–N$_d$ transition can be expected to become stronger at any given pressure and to occur at a lower temperature, due to higher values of both A and q.

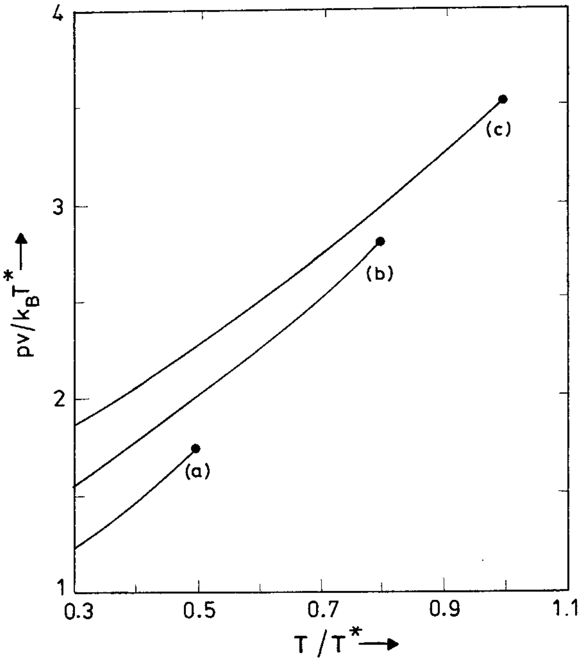

Figure 2. The p–T phase diagram for $\eta^* = 0.55$, $q = 1.2$, showing the N–N transition lines for different values of A: (*a*) $A = 3$, (*b*) $A = 5$ and (*c*) $A = 6.5$. The transition is from the N$_1$ phase (above the line) to the N$_d$ phase (below the line). The first order N$_1$–N$_d$ transition line ends in a critical point indicated by a closed circle.

We have shown in an earlier paper [14], in which the hard rod effects have not been taken into account, that a negative deviation from the geometric mean (GM) rule for the mutual interaction is *necessary* to get N_1–N_d transition and the first order nature of the N_1–N_d transition becomes stronger if the deviation is large. As discussed above, in the present calculations the hard rod effects alone are sufficient to give rise to the N_1–N_d transition even when the nematic order is saturated. Further, an increase of the chain length (i.e. q and A) has the same effect as an increase of the negative deviation. Obviously, an increase of q makes the A and P types of pairs structurally more dissimilar. From equation (13*a*), $b(q) = 0$ if $q = 1$, i.e. the two species are geometrically equivalent. Otherwise, $b(q) > 0$ which would, from equation (13), *increase* the free energy of the medium. In theories which consider only the mean field attractive part, such an increase requires a negative deviation from GM rule. Thus, the inclusion of hard rod features naturally gives rise to the observed N_1–N_d transition in the present problem. Indeed, experiments show that the N–I transition temperatures of binary mixtures of nematogens have a negative deviation from linear dependence. This has been attributed to a negative deviation from the GM rule in a theory considering only the attractive interactions [33], and later numerically shown to be equivalent to including hard rod interactions between the molecules [34]. Our present argument shows the physical origin to lie in the increase in the excluded volume ($= v[b(q) + 8]$) between cylinders of different aspect ratios, even when both of them have the *same volume.*

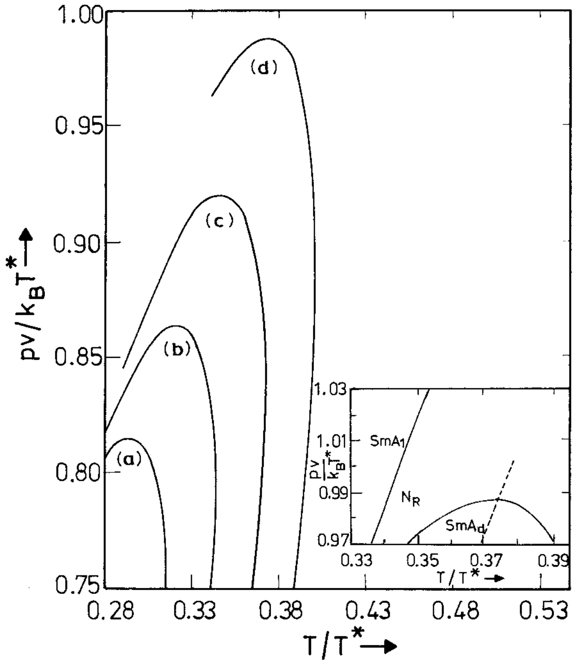

Figure 3. The p–T phase diagram obtained for $A = 1.5$, $\eta^* = 0.5$, $q = 1.8$ for different values of α_2: (*a*) $\alpha_2 = 0.048$, (*b*) $\alpha_2 = 0.054$, (*c*) $\alpha_2 = 0.06$ and (*d*) $\alpha_2 = 0.066$. The inset shows the reentrant part of the phase diagram in a magnified scale along the pressure axis for $\alpha_2 = 0.066$. The axis of the parabolic SmA_d boundary (the dotted line) and the SmA_1–N_R line are roughly parallel.

3.2. *Phase diagrams involving smectics*

3.2.1. *Double reentrance*

The packing effect alone can stabilize the smectic phase [28, 22]. However, we could not get a reentrant sequence for any combinations of $\Delta\varepsilon$ and q, by completely ignoring the attractive part of the smectic interactions. Thus, in the present model, attractive interactions between AA, PP and AP pairs are necessary to get reentrance. Relatively small values of the McMillan parameter α are sufficient to stabilize the smectic phase over wide ranges of pressure and temperature. The p–T phase diagrams obtained for $A = 1.5$, $\eta^* = 0.5$, $q = 1.8$ and α_2 varying from 0.048 to 0.066 are shown in figure 3. The SmA_d phase gets bounded in the p–T plane and its stability increases as α_2 is increased. The theoretical curves are very similar to the experimental data on mixtures of 6OCB and 8OCB studied by Cladis [18]. Higher values of α_2 correspond to larger concentrations of 8OCB which has the longer chain length. The inset also shows both the SmA_1–N_R as well as the SmA_d–N transition lines in the p–T plane for $\alpha_2 = 0.066$. The 6OCB–8OCB mixture does not exhibit the SmA_1 phase before it crystallizes. However, the theoretical diagram resembles the experimental one [18] on a compound exhibiting a double reentrant sequence. The axis of the parabolic SmA_d boundary and the SmA_1–N_R line are roughly parallel as in the experimental curve [18]. However, the pressure values are underestimated in our theory by a factor of about 4. The reason for this discrepancy is that the hard core interactions are limited to the second virial term and such an approximation is known to underestimate the pressure even for the N–I transition [35].

3.2.2. *Double reentrance with N_1–N_d transition*

As discussed in the introduction, the N_1–N_d transition can occur in the double reentrant part of the phase diagram. Our model also predicts such a sequence even in the absence of hard core interactions [36]. There is only one experimental observation of this kind [37]. By a careful and systematic search over the appropriate domains of the model parameters, we have found a very small range over which the reentrant N_1–N_d transition occurs. Figure 4 shows the p–T phase diagram for

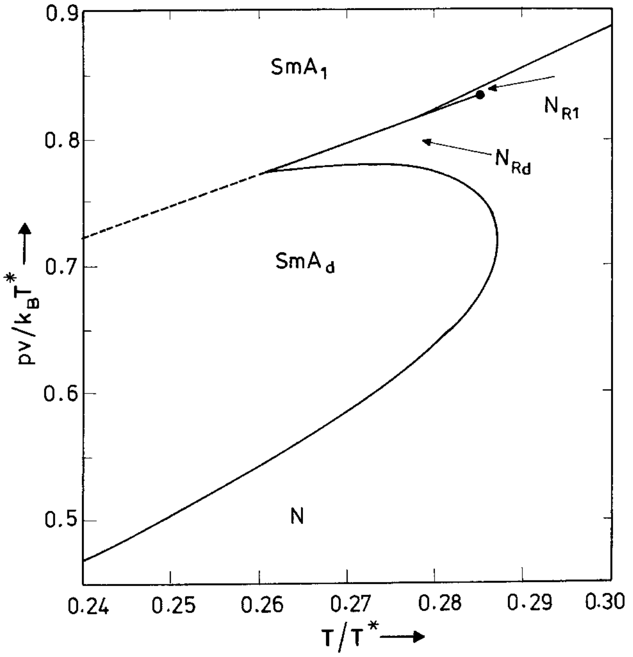

Figure 4. The p–T phase diagram obtained for $A = 1.52$, $\eta^* = 0.5$, $q = 1.8$ and $\alpha_2 = 0.042$. The values of (p, T) which are indicative of a SmA$_1$–SmA$_d$ transition are shown by a dotted line. Note that N$_{R1}$–N$_{Rd}$ transition line ending in a critical point, shown by a closed circle.

$A = 1.52$, $\eta^* = 0.5$, $q = 1.8$ and $\alpha_2 = 0.042$. As mentioned earlier, $\Delta > 0$ in equation (31) corresponds to the SmA phase. Since we have restricted the free energy expansion to the quadratic powers in the order parameters, the equations are valid only close to the N–SmA transition. Hence, we cannot locate the SmA$_1$–SmA$_d$ transition if it occurs well within the SmA phase. However, for $\Delta > 0$, at some values of (p, T) the free energies of the SmA$_1$ and SmA$_d$ phases become equal associated with a jump in x_2. This is indicative of a SmA$_1$–SmA$_d$ transition near those values of (p, T). Such values are shown with a dotted line in figure 4. The topology of the phase diagram agrees with that predicted using the dislocation loop melting theory of Prost and Toner [4]. In figure 4, the SmA$_1$–N$_{Rd}$ transition line separates the N$_{R1}$–N$_{Rd}$ transition line ending in a critical point and the SmA$_1$–SmA$_d$ transition line. Experimental data having these features in the p–T plane are not available for comparison. (However, in the temperature–concentration (T–X) plane, a diagram with a similar topology has been obtained in an experiment [37]. In an earlier paper we have shown that a similar diagram in the temperature–α plane can be obtained in a calculation in which the hard rod effects are ignored [36].) As the chain length is increased in a homologous series, $\Delta\varepsilon$ and hence A increase as mentioned earlier. The effect of this dependence is discussed in the next section.

3.2.3. *Effect of variation of* $\Delta\varepsilon$

Since from equation (1) $\Delta\varepsilon \propto A$, we have calculated the phase diagram as a function of pressure and A. The p–A phase diagram showing a reentrant nematic lake (which also has the N$_{R1}$–N$_{Rd}$ transition line changing over to the SmA$_1$–SmA$_d$ transition line) is obtained for $\eta^* = 0.5$, $q = 1.8$, $T_R = 0.28$, $\alpha_2 = 0.0475$ (figure 5). Experimentally Cladis and Brand [38] discovered long ago the SmA$_1$–SmA$_d$ transition line which ended in a (chiral) nematic lake in a binary mixture. The effect of pressure on such a phase diagram appears not to have been studied as yet, though the lake has been found in other temperature–concentration phase diagrams [39]. It may be noted that the nematic lake predicted by the frustrated spin gas model [6] is not associated with the SmA$_1$–SmA$_d$ transition line [39]. We see that, when A (i.e. $\Delta\varepsilon$ and hence the chain length) is small, as the pressure is increased, x_2 remains large till the pressure is quite high. At still higher pressures, though x_2 decreases, the high pressure is sufficient to stabilize the SmA$_1$ phase. Hence there is no N$_R$. For intermediate values of A, the value of $\Delta\varepsilon$ is large enough to cause a steeper variation of x_2 with respect to η (and hence p) around $\eta = \eta^*$. Since the A and P types of pairs are now considerably dissimilar, when x_2 decreases rapidly, the SmA$_d$ phase becomes unstable due to packing reasons and the nematic phase reenters. For higher pressures,

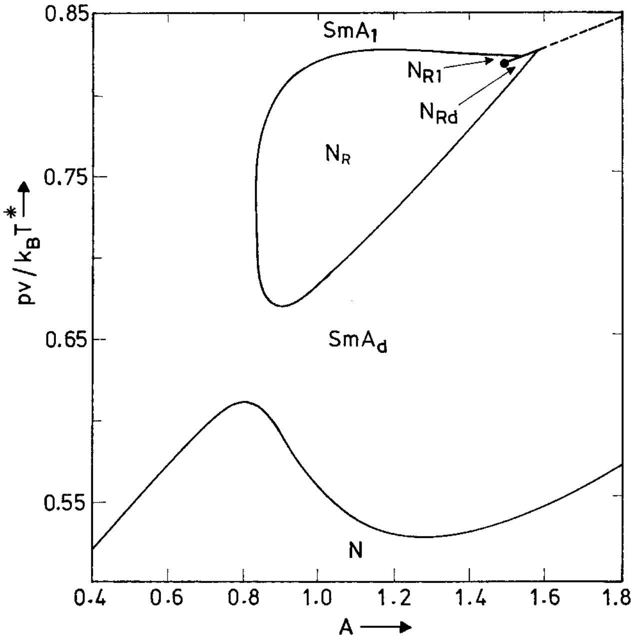

Figure 5. The p–A phase diagram showing a reentrant nematic (N$_R$) lake having the N$_{R1}$–N$_{Rd}$ transition line for $\eta^* = 0.5$, $q = 1.8$, $T_R = 0.28$, $\alpha_2 = 0.0475$. The values of (p, T) which are indicative of a SmA$_1$–SmA$_d$ transition are shown by a dotted line. The closed circle indicates the N$_{R1}$–N$_{Rd}$ critical point.

when x_1 is large, the SmA_1 phase becomes stable. For larger values of A and hence $\Delta\varepsilon$, x_2 varies quite steeply. Therefore, upto $\eta = \eta^*$, x_2 is large and for $\eta > \eta^*$, x_1 becomes large. In both cases, the SmA phase is stable due to better packing of similar molecules. Around $\eta \approx \eta^*$, there is a jump in x_2 (and hence η) which is an indication of SmA_d–SmA_1 transition (shown by dotted line).

Both $\Delta\varepsilon$ and α vary with chain length, and we have shown in an earlier paper [13] that α can be assumed to vary as $(\Delta\varepsilon)^{1/4}$. Using this variation, we have obtained a similar N_R lake in the T–α plane [13] considering only attractive interactions. In the present calculations, we get the N_R lake due to hard rod effects alone without including the variation of α with A (and hence $\Delta\varepsilon$). In principle, as the chain length is varied, $\Delta\varepsilon$, α and q vary together. Calculations including all these dependences are somewhat involved and have not been carried out.

Variation of A implies a variation of chain length, which crudely reflects the variation of concentration (X) in a binary mixture of homologues. Hence, the calculation p–A diagram can be compared with p–X diagrams. Experimentally, phase diagrams in only the p–T and T–X plane have been reported. As α_2 is decreased and other parameters kept fixed, the N_R lake widens and opens up as shown in figure 6 for $\alpha_2 = 0.047$. Also as the N_R region becomes bounded for higher values of A, the SmA_1–N_{R1} and the N_{Rd}–SmA_d lines do not meet the N_{R1}–N_{Rd} line at the same point. They are separated by the SmA_1–N_{Rd} line. The topologies of the phase diagrams (figures 5 and 6) agree quite well with the diagrams predicted by the dislocation loop melting theory of Prost and Toner (see figure 10.34 in [1]). As mentioned earlier, experimental p–X diagrams are not available for comparison. However, in T–X diagrams a similar topology has been noted [37]. If α_2 is increased to 0.05, the nematic lake shrinks and the N_{R1}–N_{Rd} line is not seen as an extension of the SmA_1–SmA_d line.

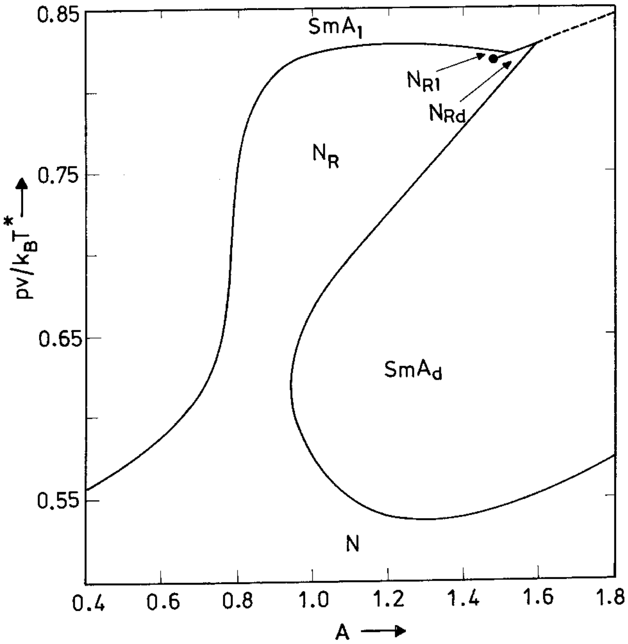

Figure 6. The p–A phase diagram for $\eta^* = 0.5$, $q = 1.8$, $T_R = 0.28$, $\alpha_2 = 0.047$, showing the opening of the reentrant nematic lake of figure 5 creating a 'bay'. The values of (p, T) which are indicative of a SmA_1–SmA_d transition are shown by a dotted line. The closed circle indicates the N_{R1}–N_{Rd} critical point.

Quadruple reentrance is a very rare phenomenon and is seen only in one compound [40]. The phenomenon has been predicted by both the dislocation loop melting theory [4] and the spin gas theory [6]. The compound used in reference [40] is DB_nONO_2 which has the chemical formula $C_nH_{2n+1}O$–ϕ–OOC–ϕ–OOC–ϕ–NO_2 where ϕ denotes a phenyl ring and n is the number of carbon atoms in the alkyl chain. This compound has a terminal nitro dipole which is oppositely oriented to the two ester dipoles in the core. Hence, antiparallel configurations with different extents of overlappings are possible resulting in smectic polymorphism. This requires a model considering antiparallel configurations with different lengths and configurational energies which is obviously very involved. However, in our simple model, the possibility of quadruple reentrance at a constant pressure is already seen in the upper part of figure 6. For clarity, this part is shown in a magnified scale along the pressure axis (figure 7). As A is decreased, the phase sequence of SmA_d–N_{Rd}–SmA_1–N_{R1}–SmA_1 occurs along the dotted line. It can be noted that the quadruple reentrance occurs only over a very small range of values of the model parameters.

4. Conclusions

We have extended our earlier model [13] developed to explain double reentrance to include hard core interactions, adopting the method used by Koda and Kimura [22]. Assuming perfect orientational order, we have calculated pressure–temperature phase diagrams showing nematic to nematic (N_1–N_d) transition, double reentrance with bounded SmA_d region and N_1–N_d transition associated with double reentrance. We have also calculated pressure versus A (a parameter which increases with the chain length in a homologous series) phase diagrams. These show the reentrance nematic (N_R) lake associated with the SmA_1–SmA_d transition, N_1–N_d transition occurring inside such an N_R lake, quadruple reentrance at constant pressure, and widening and merging of the N_R lake with the main nematic sea. The results are compared with other theories and the available experimental data. Our results confirm that the hard core interaction is the physical origin for the effective

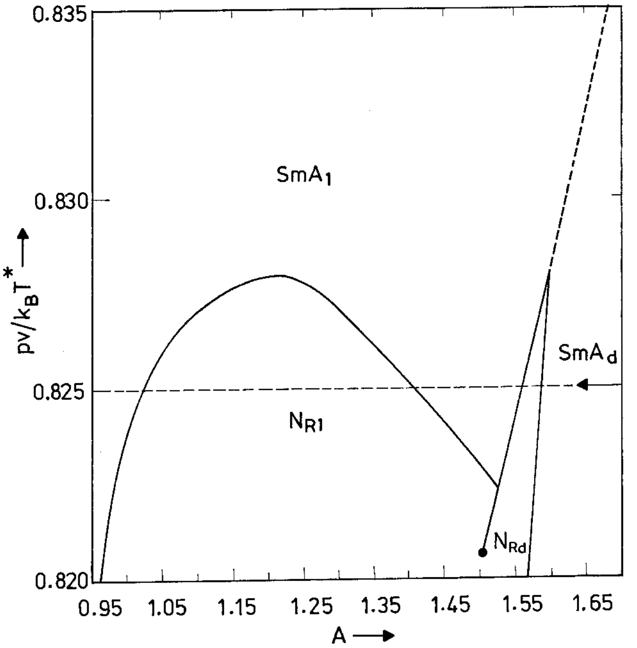

Figure 7. The upper part of figure 6 is shown in a magnified scale along the pressure axis. As *A* is decreased, the quadruple reentrant phase sequence SmA$_d$–N$_{Rd}$–SmA$_1$–N$_{R1}$–SmA$_1$ as indicated by the dotted line becomes possible. The closed circle indicates the N$_{R1}$–N$_{Rd}$ critical point.

mutual interaction between A and P types of pairs, being less than that obtained as the geometric mean of the individual attractive interactions, and this effect increases as the two components become structurally more dissimilar. Also, in general as the chain length is increased, if the smectic phase does not intervene, the first order nature of the N$_1$–N$_d$ transition can be expected to become stronger at any given pressure and to occur at a lower temperature. Further, the stability of the SmA$_d$ phase increases, i.e. it gets bounded at higher pressures, as the chain length increases as seen experimentally.

References

[1] De Gennes, P. G., and Prost, J., 1993, *The Physics of Liquid Crystals*, 2nd Edn (Oxford Science Publications).

[2] Cladis, P. E., 1999, in *Physical Properties of Liquid Crystals*, edited by D. Demus, J. Goodby, G. W. Gray, H.-W. Spiess, and V. Vill (Wiley-VCH) p. 290.

[3] Barois, P., Prost, J., and Lubensky, T. C., 1985, *J. Phys.*, **46,** 391.

[4] Prost, J., and Toner, J., 1987, *Phys. Rev. A*, **36,** 5008.

[5] Longa, L., and de Jeu, W. H., 1981, *Phys. Rev. A*, **26,** 1632.

[6] Marko, J. F., Indekeu, J. O., and Berker, A. N., 1989, *Phys. Rev. A*, **39,** 4201.

[7] Dowell, F., 1987, *Phys. Rev. A*, **36,** 5046.

[8] Mirantsev, L. V., 1986, *Mol. Cryst. liq. Cryst.*, **133,** 151.

[9] Katriel, J., and Kvenstel, G. F., 1985, *Mol. Cryst. liq. Cryst.*, **124,** 179.

[10] Bose, T. R., Mukherjee, C. D., Roy, M. K., and Saha, M., 1985, *Mol. Cryst. liq. Cryst.*, **126,** 197.

[11] Hida, K., 1981, *J. phys. Soc. Jpn.*, **50,** 3869.

[12] Madhusudana, N. V., and Rajan, J., 1990, *Liq. Cryst.*, **7,** 31.

[13] Govind, A. S., and Madhusudana, N. V., 1997, *Liq. Cryst.*, **23,** 327.

[14] Govind, A. S., and Madhusudana, N. V., 1993, *Liq. Cryst.*, **14,** 1539.

[15] Basappa, G., Govind, A. S., and Madhusudana, N. V., 1997, *J. Phys. II Fr.*, **7,** 1693.

[16] Madhusudana, N. V., and Chandrasekhar, S., 1973, *Pramana Suppl.*, **1,** 57.

[17] Basappa, G., and Madhusudana, N. V., 1998, *Eur. Phys. J. B*, **1,** 179.

[18] Cladis, P. E., 1980, in *Liquid Crystals*, edited by S. Chandrasekhar (London: Heyden), p. 105.

[19] Cladis, P. E., Bogardus, R. K., Daniels, W. B., and Taylor, G. N., 1977, *Phys. Rev. Lett.*, **39,** 720.

[20] Clark, N. A., 1979, *J. Phys.*, **40,** C3-345.

[21] Sear, R. P., and Jackson, G., 1995, *Phys. Rev. Lett.*, **74,** 4261.

[22] Koda, T., and Kimura, H., 1994, *J. Phys. Soc. Jpn.*, **63,** 984.

[23] Onsager, L., 1949, *Ann. N. Y. Acad. Sci.*, **51,** 627.

[24] Stroobants, A., Lekkerkerker, H. N. W., and Frenkel, D., 1986, *Phys. Rev. Lett.*, **57,** 1452; Stroobants, A., Lekkerkerker, H. N. W., and Frenkel, D., 1987, *Phys. Rev. A*, **36,** 2929.

[25] Watanabe, J., and Takashina, Y., 1991, *Macromolecules*, **24,** 3423.

[26] Hosino, N., Nakano, H., and Kimura, H., 1979, *J. phys. Soc. Jpn.*, **47,** 740.

[27] Mulder, B., 1987, *Phys. Rev. A*, **35,** 3095.

[28] Wen, X., and Meyer, R. B., 1987, *Phys. Rev. Lett.*, **59,** 1325.

[29] Taylor, M. P., Hentschke, R., and Herzfeld, J., 1989, *Phys. Rev. Lett.*, **62,** 800.

[30] Nakagawa, M., and Akahane, T., 1985, *J. phys. Soc. Jpn.*, **54,** 69.

[31] Warrier, S. R., Vijayaraghavan, D., and Madhusudana, N. V., 1998, *Europhys. Lett.*, **44,** 296.

[32] Manjuladevi, V., and Madhusudana, N. V. (to be published).

[33] Humphries, R. L., James, P. G., and Luckhurst, G. R., 1971, *Symp. Faraday Soc.*, **5,** 107.

[34] Nakagawa, M., and Akahane, T., 1983, *J. phys. Soc. Jpn.*, **52,** 399.

[35] Mulder, B. M., and Frenkel, D., 1985, *Mol. Phy.*, **55,** 1193.

[36] Govind, A. S., and Madhusudana, N. V., 2000, *Liq. Cryst.*, **27,** 215.

[37] Nounesis, G., Kumar, S., Pfeiffer, S., Shashidhar, R., and Garland, C. W., 1994, *Phys. Rev. Lett.*, **73,** 565.

[38] Cladis, P. E., and Brand, H. R., 1984, *Phys. Rev. Lett.*, **52,** 2261.

[39] Wu, L., Garland, C. W., and Pfeiffer, S., 1992, *Phys. Rev. A*, **46,** 973.

[40] Raja, V. N., Ratna, B. R., Shashidhar, R., Heppke, G., Bahr, Ch., Marko, J. F., Indekeu, J. O., and Berker, A. N., 1989, *Phys. Rev. A*, **39,** 4341.